(Semi-)Quantitative Analysis of Reduced Nicotinamide Adenine Dinucleotide Fluorescence Images of Blood-Perfused Rat Heart

J. M. C. C. Coremans,* C. Ince,*# H. A. Bruining,* and G. J. Puppels*
*Department of General Surgery, Erasmus University Rotterdam, Rotterdam, and #Department of Anaesthesiology, University of Amsterdam, Amsterdam, The Netherlands

ABSTRACT In vivo analysis of the metabolic state of tissue by means of reduced nicotinamide adenine dinucleotide (NADH) fluorimetry is disturbed by tissue movements and by hemodynamic and oximetric effects. These factors cause changes in the absorption of ultraviolet (UV) excitation light by the tissue. Many different methods have been used in the literature to compensate measured NADH fluorescence intensities for these effects. In this paper we show on theoretical grounds that the ratio of NADH fluorescence intensity and UV diffuse reflectance intensity provides a (semi-)quantitative measure of tissue NADH concentrations. This result is corroborated by experiments with tissue phantoms in which absorption and backscattering properties were varied. Furthermore, we have verified the validity of this compensation method in isolated Langendorff-perfused rat heart preparations. In this preparation oximetric effects (of blood and tissue) are the major determinants of the metabolism-dependent UV diffuse reflectance change. Hemodynamic effects accompanying compensatory vasodilation are negligible. Movement artifacts were eliminated by simultaneously recording fluorescence and reflectance images, using a CCD camera with a biprism configuration. The results show that the NADH fluorescence/UV reflectance ratio can be used to monitor the mitochondrial redox state of the surface of intact blood-perfused myocardium.

INTRODUCTION

Intraoperative assessment of hypoxic areas in myocardium can yield important information during, e.g., by-pass surgery. In general, knowledge of the adequacy of O_2 delivery by the circulation to the mitochondria in tissue is crucial in clinical diagnosis. In mitochondria, the major net energy conversion is based on electron transport from reduced nicotinamide adenine dinucleotide (NADH) to molecular O_2 via a series of catabolic reactions in the respiratory chain. Hence the NADH/NAD^+ redox couple reflects the mitochondrial redox state and cellular hypoxia, when oxidative phosphorylation is curtailed by insufficient O_2. NADH, unlike its conjugated electron acceptor NAD^+, fluoresces in the blue (broad-band emission centered around 460 nm) upon excitation with ultraviolet (UV) light. Therefore the fluorescent property of NADH may be used to monitor cellular metabolism, as was first pointed out by Chance et al. (Chance and Thorell, 1959).

The blue autofluorescence of different cell types can only be used as an indicator of cellular hypoxia when mitochondrial NADH is the dominant intrinsic fluorescent probe (Chance et al., 1962). For heart tissue it has been shown that the blue autofluorescence is primarily of mitochondrial origin, with insignificant contributions of cytoplasmic fractions (Jöbsis and Duffield, 1967; Nuutinen, 1984; Eng et al., 1989). Because NADH is the predominant reduced pyridine nucleotide in mitochondria of heart (Klingenberg et al., 1959) and the fluorescent yield of NADH is three to four times higher than that of reduced nicotineamide adenine dinucleotide phosphate (NADPH) (Avi-Dor et al., 1962; Estabrook, 1962; Jöbsis and Duffield, 1967), the contribution of NADPH to the measured blue autofluorescence of heart tissue is negligible. The UV-induced blue fluorescence of collagen and fat is independent of the tissular redox/oxygenation state and therefore does not disturb the evaluation of the metabolic state of tissue (Deyl et al., 1969; Pappajohn et al., 1972; Schomacker et al., 1992).

In spite of the potential of NADH fluorimetry for a noninvasive diagnostic approach, clinical application of the technique has been limited because of the problems involved in quantitative analysis of the NADH redox state (Duboc et al., 1986, 1987; Renault et al., 1987; Austin et al., 1978). Several physiological factors that affect fluorescence intensity must be taken into account (Ince et al., 1992). In organs and tissues with an intact blood supply, absorption of fluorescence excitation and emission light by blood pigments (hemoglobin) results in a hemoglobin concentration-dependent reduction of NADH fluorescence intensity (hemodynamic effect). The absorption spectra of hemoglobin and tissue pigments (e.g. myoglobin, cytochromes) depend on their oxygenation/redox state. Hence NADH fluorescence intensity is also affected by metabolic state-related changes in the spectral characteristics of these pigments (oximetric effect) (Coremans et al., 1993). In addition, tissue movement can easily alter the amount of specular reflection of UV excitation light at the air-tissue interface and thereby the effective UV excitation intensity in the tissue. The extent to which these effects interfere with NADH fluorescence measurements is dependent on the organ under investigation.

Received for publication 24 June 1996 and in final form 23 December 1996.

Address reprint requests to Dr. J. M. C. C. Coremans, Department of General Surgery, University Hospital Rotterdam, dr Molewaterplein 40, 3015 GD Rotterdam, The Netherlands. Tel.: 31-10-4087762; Fax: 31-10-4369140; E-mail: coremans@lchir.fgg.eur.nl.

0006-3495/97/04/1849/12 $2.00

Over the past 25 years several methods have been proposed to correct measured NADH fluorescence intensities for light absorption by the tissue that is investigated, to obtain (semi-)quantitative information on the mitochondrial redox state (Ince et al., 1992). Most methods utilized a light reflectance measurement at a certain wavelength to monitor changes in optical properties of the tissue surface (Dóra et al., 1984; Harbig et al., 1976; Ji et al., 1977, 1979; Jöbsis et al., 1971; Kobayashi et al., 1971; Kovach et al., 1977; Mayevsky and Chance, 1974, 1982; Mayevsky et al., 1987; Mills et al., 1977; Osbakken, 1994; Renault et al., 1984), but fluorescence measurements have also been used (Heineman and Balaban, 1990; Koretsky et al., 1987; Kramer and Pearlstein, 1979; Vern et al., 1975). When the oximetric effect was regarded to be of minor importance, the intensity of the reflected excitation light (365 nm) was subtracted from the measured fluorescence signal to obtain corrected NADH fluorescence intensities (Dóra et al., 1984; Harbig et al., 1976; Ji et al., 1977; Jöbsis et al., 1971; Mayevsky and Chance, 1974, 1982; Mayevsky et al., 1987; Kovach et al., 1977; Osbakken, 1994). In case the oximetric effect of hemoglobin was considered to significantly disturb the fluorescence measurement, reflectance measurements were carried out at isosbestic wavelengths of hemoglobin (e.g., 586 nm (Renault et al., 1984), 720 nm (Kobayashi et al., 1971). Others have recorded the blue NADH fluorescence at isosbestic wavelengths of hemoglobin (e.g., 445 nm, Harbig et al., 1976; 448 nm, Kramer and Pearlstein, 1979).

To suppress the effect of motion on NADH fluorimetry of heart, fluorescence emission ratios (Brandes et al., 1992) and fluorescence excitation ratios (Scott et al., 1994) have been suggested. These methods, however, were not developed to account for hemodynamic and oximetric effects on the absorption of NADH fluorescence excitation and emission light by the tissue.

For rat heart, the relative difference in NADH fluorescence intensity between hypoxic and normoxic tissue in vivo is smaller than the corresponding difference in fluorescence intensity found in vitro (see, e.g., below, Fig. 7). Nevertheless, enhanced NADH fluorescence intensity during hypoxia remains clear (see below, Fig. 6, and Ince and Bruining, 1991), despite compensatory vasodilation and oximetric effects of blood and tissue in blood-perfused heart. Earlier investigations, in which NADH videofluorimetry was used in combination with diffuse reflectance spectroscopy (400–700 nm), have shown that the reduction of the NADH fluorescence intensity difference between hypoxic and normoxic tissue in vivo is not due to increased absorption of the fluorescence light (Coremans et al., 1993). This implies that the decrease in NADH fluorescence intensity difference in vivo is caused by reduced NADH fluorescence excitation efficiency under hypoxic conditions.

We have investigated the use of diffuse reflectance measurements at the excitation wavelength (365 nm) for the correction of measured NADH fluorescence intensities. It is shown, both on theoretical grounds and by experiments on tissue phantoms and freshly excised rat hearts, that the ratio of simultaneously measured NADH fluorescence image intensities and UV reflectance image intensities provides an adequate correction for the influence of hemodynamic effects, oximetric effects, and tissue movements on measured NADH fluorescence intensities. Therefore this ratio can be used to obtain semiquantitative information about the mitochondrial redox state of surface layers of intact myocardium in vivo.

MATERIALS AND METHODS

All experiments described in this paper were performed according to experimental protocols, which were approved by the Internal Animal Care and Use Comittee of the Erasmus University Rotterdam.

Optics

Similar to the fluorimeter described by Vern et al. (1975), a biprism (3° wedge, fused silica; Melles Griot B.V., Zevenaar, The Netherlands) was used for simultaneous projection of NADH fluorescence and UV reflectance images on the CCD chip of a video camera (Fig. 1). We have used a second-generation CCD video camera (MXRi; Adimec Advanced Image Systems B.V., Eindhoven, The Netherlands), equipped with an ultraviolet blue-sensitive S20 photocathode (Philips, Eindhoven, The Netherlands) and a Micro-Nikkor 105-mm macro lens. The videofluorimeter with which the NADH fluorescence image in Fig. 4 was recorded has been described in detail (Coremans et al., 1993; Ince et al., 1993).

UV excitation light of 365 nm was provided by a 200-W xenon mercury lamp (Universal arc lamp source 66006, F/1.5 single element fused silica condenser; Oriel, Stratford, CT) and selected by means of a UG-1 color glass filter (Oriel). The intensity of the excitation light ($\leq$1 mW/cm^2) was not able to excite all of the NADH molecules in the surface layers of intact myocardium. A linear relationship was found between the intensities of NADH fluorescence excitation and emission light, when the intensity of

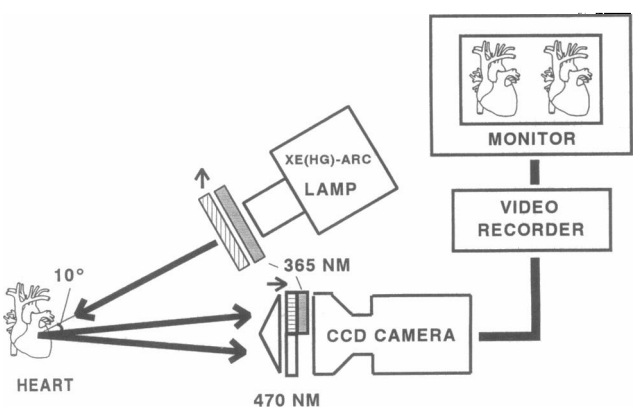

FIGURE 1 Schematic representation of the experimental set-up for simultaneous measurement of NADH fluorescence (±470 nm) and UV reflectance (365 nm) images. Images are recorded with a second-generation image-intensified CCD video camera equipped with a 105-mm macro lens. Excitation light at 365 nm, which is provided by a 200-W xenon mercury lamp, is selected by means of an UG-1 color glass filter. NADH fluorescence is selected from the emitted tissue fluorescence by a 470-nm narrow-band interference filter. A biprism (3° wedge) is used to enable simultaneous measurement of NADH fluorescence and diffuse UV reflectance images of rat heart. To prevent contributions of specularly reflected UV light to the diffuse reflectance image, a crossed polarizer/analyzer combination is used.

UV excitation light was varied (0–100%) with a set of neutral density filters.

One half of the biprism was covered with an interference filter for transmission of NADH fluorescence (470 nm, BWHM 10 nm; Melles Griot). The other half of the biprism was covered with another UG-1 filter for transmission of reflected UV excitation light. Reflectance measurements of a spherical and beating heart are complicated by the presence of signal contributions due to specularly reflected UV light. We have eliminated this unwanted contribution of specularly reflected excitation light to the UV reflectance image by means of a crossed polarizer/analyzer combination (Polaroid Type HNP'B Linear polarizer; Polarizer Division, Hertfordshire, England). Specularly reflected, linearly polarized excitation light preserves its polarization and is blocked by the analyzer. Diffusely reflected excitation light becomes depolarized because of multiple scattering of photons inside the tissue. Part of the diffusely reflected depolarized light will be transmitted by the analyzer in front of the camera lens and is used to form the reflectance image.

In some experiments reflectance measurements were carried out at both 365 nm and 586 nm. In those cases the biprism was removed and NADH fluorescence, 365 nm reflectance, and 586 nm reflectance were measured consecutively. Appropriate filter combinations were used in excitation and emission paths. Light at 586 nm was selected by means of an interference filter (586 nm, BWHM 20 nm; Chroma Technology Corp., Brattleboro, VT).

Images were video recorded (Panasonic S-VHS professional video recorder model AG-7330; Matsushita Electric Industrial Co., Osaka, Japan) and computer analyzed off-line. With image-processing software (TCL Image, Multihouse, Amsterdam, The Netherlands; Olivetti M380-XP5-386 personal computer; digitizer, Digital Production Mixer type WJ-MX10, Panasonic; frame grabber, Data Translation type DT2801, Marlboro, MA), identical tissue areas in the simultaneously recorded NADH fluorescence and diffuse UV reflectance images could be selected. The averaged intensities of these areas are displayed in Figs. 2 and 5–7.

A small circular piece of uranyl fluorescence calibration glass was placed next to the heart in the lower left corner of the excitation field (Ploem, 1970). NADH fluorescence and UV reflectance intensities of heart were related to the fluorescence intensity of this calibration glass and are expressed in arbitrary units (A.U.). The fluorescence calibration glass served as a marker for the image-processing software to select identical tissue areas in the reflectance and fluorescence image of one video frame. It was also used to monitor fluctuations in the intensity of the light source.

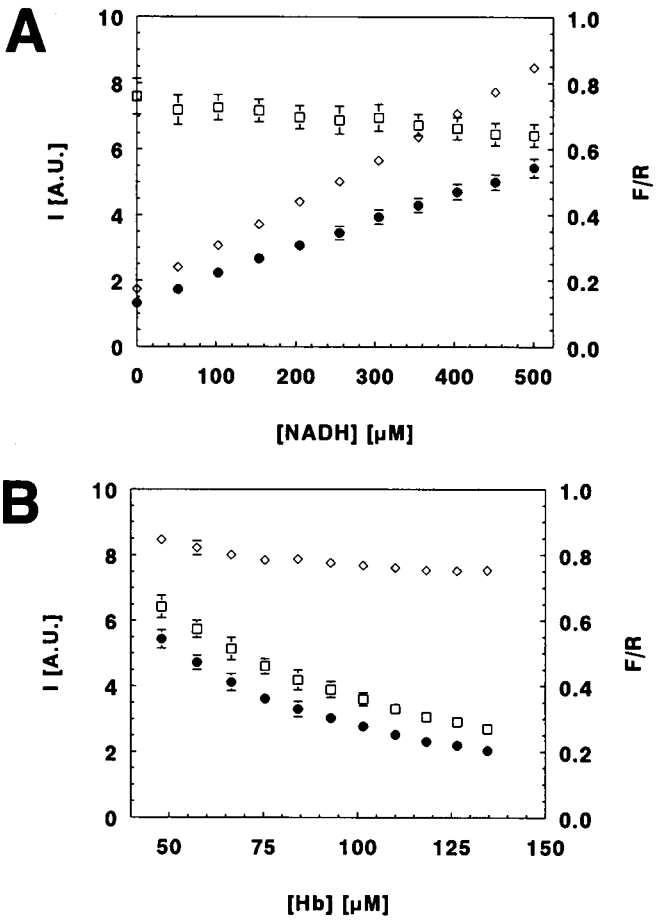

FIGURE 2 F_{NADH} intensity (●), R_{365} intensity (□), and F_{NADH}/R_{365} ratio (◇) as (*A*) a function of NADH concentration in a tissue phantom composed of 50 μM hemoglobin and Intralipid-3%. The positive intercept of the fluorescence axis is caused by Intralipid, which also fluoresces around 470 nm upon excitation with UV light. (*B*) A function of increasing hemoglobin concentration with 400 μM NADH added to the tissue phantom. A.U., Arbitrary units.

Preparation of hearts

Perfusion experiments were performed on hearts of male Wistar rats weighing 275–375 g. Rats were anesthetized by ether inhalation. After heparinization of the animal (200 IU/kg body weight iv, Heparin; Leo Pharmaceutical Products B.V., Weesp, The Netherlands), the thoracic cavity was opened by sternotomy. Hearts were excised, chilled in ice-cold Tyrode, and immediately transferred to a Langendorff set-up. In a Langendorff preparation the perfusate leaves the coronary vascular system at the coronary sinus and the opened right atrium and drips off the apex of the heart. In blood perfusion experiments a film of perfusate on the heart surface would interfere with our measurements. In that case, all efferent vessels were closed, except for one pulmonary artery, which was cannulated with fine-bore polythene tubing for drainage (800/100/240/100: Portex, Hythe, England). Hearts were allowed to beat freely. No special precautions were taken to control the oxygenation of the ambient gas phase.

For in vivo measurements rats were anesthetized by ether inhalation and heparinized. After tracheotomy the rats were mechanically ventilated (Loosco, Amsterdam MK2 infant ventilator, The Netherlands) with 65% O_2, 32.5% N_2O, and 2.5% of the anesthetic ethrane. To create hypoxic hypoxia, N_2 was substituted for O_2 in the respiratory gas. The rats were kept on a heated mat (37°C) to prevent hypothermia.

Perfusion system

The perfusion system offered the possibility to switch rapidly between four available perfusates: both oxygenated and deoxygenated Tyrode solution and oxygenated and deoxygenated suspensions of washed rat erythrocytes in Tyrode solution were used.

The Tyrode solution consisted of 128 mM NaCl, 4.7 mM KCl, 1 mM $MgCl_2$, 0.4 mM $NaH_2PO_4 \cdot H_2O$, 1.2 mM Na_2SO_4, 20.2 mM $NaHCO_3$, 1.3 mM $CaCl_2$, and 11.0 mM glucose, supplemented with 1% bovine serum albumin (BSA). This solution was filtered through a 1.2-μm filter (Schleicher and Schuell, Dassel, Germany).

Rat erythrocytes were obtained from fresh blood from five to seven anesthetized male Wistar rats, weighing 300–400 g. Anesthesia was induced by ether inhalation. After heparinization of the donor animals (280 IU/kg body weight, i.v.), blood was collected in syringes containing 50 IU heparin via punction of the abdominal aorta. Blood was centrifuged at 1500 × *g* for 10 min to remove plasma and buffy coats. The remaining cells were washed three times with Tyrode equilibrated with 95% O_2/5% CO_2 and supplemented with 0.1% BSA. Finally, the erythrocytes were suspended up to a hematocrit of 9–10% in Tyrode containing 1% BSA.

Before transfer of the erythrocyte suspension to the perfusion system, the entire flow circuit had been coated with BSA to prevent damage to the erythrocytes by shear forces. To each reservoir containing erythrocyte

suspension, 170 IU heparin was added. Occasional cell aggregates were removed from the suspension by an extracorporeal blood filter (peadiatric size LPE 1440; Pall Biochemical Limited, Portsmouth, England). The erythrocyte suspension was checked regularly for hemolysis and changes in composition with a Sysmex microcell counter F-800 (TOA Medical Electronics Co., LTO, Kobe, Japan). The oxygenated erythrocyte suspension was equilibrated with 95% air/5% CO_2, and oxygenated Tyrode was equilibrated with 95% O_2/5% CO_2. In the following, the erythrocyte suspension will be referred to as *blood*. Deoxygenated perfusates were equilibrated with 95% N_2/5% CO_2. pH, pO_2, and pCO_2 of the perfusates were monitored by an AVL 945 automatic blood gas system (AVL LIST GmbH, Medizintechnik, Graz, Austria). When necessary, pH was adjusted by bicarbonate addition. Perfusates were thermostatted at 37°C, and aortic pressure was set at 60 mm Hg. Mean coronary flow was measured just in front of the aortic cannula with an in-line flow probe, operating on the ultrasonic transit-time principle (T106; Transonic Systems, New York).

Experimental protocols

Although hemodynamic and oximetric changes are linked physiological responses, experimental protocols were designed to separate the contributions of hemodynamic and oximetric changes and to discriminate between blood and tissue oxygenation changes. Four distinct protocols were used: I, II, and III (see below) were performed on isolated rat heart; protocol IV was performed on rat heart in vivo.

After arrangement for Langendorff perfusion with oxygenated Tyrode, hearts were allowed to stabilize for 30 min. In the *blood* perfusion protocols II and III, hearts were immediately perfused with oxygenated erythrocyte suspension after attachment to the aortic cannula. All other preparative steps were performed on the *blood*-perfused organ. After completion of the cannulation procedure, hearts were allowed to adjust to perfusion conditions for at least 30 min.

Protocol I was used to assess the metabolic state-related change in absorption of heart tissue (oximetric effect of tissue) at the excitation wavelength (365 nm) and at an isosbestic wavelength for hemoglobin (586 nm). In Tyrode-perfused oxygenated hearts, hypoxic hypoxia was induced by perfusion with deoxygenated Tyrode for 2.5 min. Upon return to perfusion with oxygenated Tyrode, the normoxic state was recovered. Perfusion with oxygenated Tyrode was maintained for 10 min. This cycle of hypoxia and normoxia was performed for the NADH fluorescence measurement and the reflectance measurements at 365 nm and 586 nm each.

Protocol II was used to investigate the effect of absorption and scattering properties of erythrocytes on NADH fluorescence and UV reflectance intensities under normoxic and ischemic conditions. To this end oxygenated *blood* was replaced with oxygenated Tyrode for 30 s. Three consecutive Tyrode flushes, spaced 1 min apart, were performed. After the Tyrode flushes and a stabilization interval of 6 min, the supply of oxygenated *blood* was interrupted for 1 min. Reoxygenation with *blood* was sustained for 5 min before a second ischemia/recovery cycle was performed. Subsequently, the perfusate was temporarily switched to oxygenated Tyrode for another ischemia/reperfusion cycle.

Protocol III served to estimate the relative contribution of oximetric changes and hemodynamic changes accompanying compensatory vasodilation to the fluorescence and reflectance measurements. In *blood*-perfused hearts hypoxic hypoxia was induced by replacing oxygenated perfusate with deoxygenated perfusate for 10 min. O_2 supply was restored by perfusion with oxygenated *blood* for 10 min.

Protocol IV was used to establish NADH fluorescence and 365-nm and 586-nm reflectance changes during hemodynamic and oximetric changes in vivo. To this end, three consecutive cycles of hypoxic hypoxia were created by replacing O_2 with N_2 in the respiratory mixture for 2 min.

Tissue phantom experiments

A mixture of Intralipid and soluble absorbers was used to simulate the optical properties of heart tissue (Flock et al., 1992; Staveren et al., 1991). The addition of hemoglobin was used to mimick changing tissue absorbance. Varying concentrations of NADH and/or bovine hemoglobin were added to stirred 3-ml quartz cuvettes (1-cm path length), filled with Intralipid 3% or Intralipid 6% in saline. NADH and hemoglobin were prepared as concentrated stock solutions in saline. With this method the final dilution of the Intralipid suspension by NADH and/or hemoglobin addition never exceeded 3.5%.

Optical parameters of tissue phantoms and rat heart

To verify the suitability of hemoglobin/Intralipid suspensions as tissue phantoms for rat heart, the absorption coefficient μ_a and the reduced scattering coefficient $\mu_s' = \mu_s(1 - g)$ were measured at room temperature in the UV-spectral region (331, 351, 364 nm) with a double-integrating sphere system as described by Pickering et al. (1993).

Reflectance and diffuse transmittance of the sample, which was placed between the two integrating spheres, were measured by photodiodes (EG&G Princeton Applied Research UV100BQ). A photomultiplier tube (Hamamatsu, R928) was used to collect the collimated transmittance. A 1-mm collimated beam of the UV multiline (331, 351, 364 nm) of an argon ion laser (Spectra Physics model 20) was used to irradiate the sample. To avoid contributions of UV-induced fluorescence, UG-1 filters were placed in front of each detector. The use of polychromatic light prevents separation of the reduced scattering coefficient into the scattering coefficient μ_s and the anisotropy of scattering g. An inverse adding doubling algorithm was used to solve the radiative transfer equation (Prahl et al., 1993).

Freshly excised rat hearts ($n = 9$) were flushed with saline and cut into slices. For each heart several slabs were positioned in a glass sample holder, ensuring that the sample port was completely covered (average sample thickness 427 ± 45 μm, $n = 9$). Refractive index mismatch between sample and glass was minimized by a drop of saline. With this type of preparation it was not possible to poise the oxygenation/redox state of the examined heart tissue.

A flow cuvette was used (sample thickness 500 μm) for measurement of the optical properties of both oxygenated and deoxygenated blood. The flow circuit, which consisted of the cuvette, a silicon membrane oxygenator (Alexander et al., 1984; Hamilton et al., 1974), and a bubble trap, was coated with BSA through circulation of a Tyrode solution supplemented with 1% BSA. Just before the addition of freshly collected rat blood, 170 IU heparin was added to the flow circuit. To allow transmission measurements, blood was diluted to a hematocrit of either 5.4% or 2.5%. Oxygenated blood was equilibrated with 95% O_2/5% CO_2; deoxygenated blood was equilibrated with 95% N_2/5% CO_2.

Optical properties of Intralipid (3% or 6%) with 50, 100, or 200 μM hemoglobin were determined for both 300-μm and 400-μm sample thicknesses.

NADH (grade II) was obtained from Boehringer (Mannheim, Germany), Intralipid 10% from Kabi Pharmacia AB (Sweden). Hemoglobin and BSA (fraction V) were obtained from Sigma Chemical Company (St. Louis, MO), and the constituents of Tyrode were obtained from Merck (Darmstadt, Germany).

RESULTS

Theory

For description of the radiation transfer involved in NADH fluorimetry of rat heart, the theories of front-face fluorimetry (Eisinger and Flores, 1979) and Kubelka and Munk (Kubelka, 1948, 1954; Kubelka and Munk, 1931) were combined.

Front-face fluorimetry refers to the geometry that is used primarily in studies of solid samples in which the excitation light and emitted fluorescence light enter and leave the same

sample face. Regarding the NADH fluorescence measurement of myocardial tissue, this requires that the UV excitation light (intensity, I_{ex}) is absorbed within a sample depth less than the thickness of the myocardial wall (d). The optical penetration depth for UV excitation light (δ) is defined as the distance over which the total fluence rate ($W \cdot mm^{-1}$) drops to e^{-1} (Svaasand and Ellingsen, 1983). The condition that must be fulfilled is therefore

$$d/\delta \gg 1. \quad (1a)$$

In terms of optical properties:

$$d/\delta = d \cdot \{3\mu_a(\mu_a + (1 - g)\mu_s)\}^{1/2} \gg 1, \quad (1b)$$

where δ is given by $\{3\mu_a(\mu_a + (1 - g)\mu_s)\}^{-1/2}$, μ_a is the absorption coefficient (mm^{-1}), μ_s is the scattering coefficient (mm^{-1}), and g is the anisotropy factor (Ishimaru, 1978).

Under this condition, NADH fluorescence intensity of myocardial tissue (F_{NADH}) is proportional to the ratio A_{NADH}/A_T, where A_T is total absorbance and A_{NADH} is absorbance by NADH (Eisinger and Flores, 1979):

$$F_{NADH} = G\phi(A_{NADH}/A_T)I_{ex}, \quad (2)$$

where G is a geometrical factor characteristic for the instrument, and ϕ is the fluorescence quantum yield of NADH.

From the theory of Kubelka and Munk (Kubelka, 1948, 1954), a relationship can be derived between the total sample absorbance A_T, scattering S, and diffuse UV reflectance R_{365} (Kessler and Frank, 1992):

$$A_T/S = 0.5\, R_{365}/I_{ex} + I_{ex}/R_{365} - 1. \quad (3)$$

At sufficiently high absorbance, the right-hand side of Eq. 3 will be dominated by the second term, and the ratio of absorption to scattering becomes inversely proportional to the reflectance intensity:

$$A_T/S \propto I_{ex}/R_{365}. \quad (4)$$

Under the assumption that the basic scattering properties of the tissue are constant (Heinrich et al., 1987; Hoffmann et al., 1983, 1984; Kessler and Frank, 1992), Eq. 4 implies that the diffuse reflectance intensity can be used to monitor changes in tissue absorbance.

Combination of expressions 2 and 4 leads to

$$F_{NADH}/R_{365} \propto C\, A_{NADH}, \quad (5)$$

with S, G, and ϕ incorporated into the constant C.

A_{NADH} is proportional to the NADH concentration. Expression 5 therefore gives a linear relationship between NADH concentration and fluorescence intensity. This makes the F_{NADH}/R_{365} ratio a highly suitable measure for semiquantitative fluorimetry.

Moreover, because A_T is eliminated in the expression for F_{NADH}/R_{365}, this ratio is independent of hemodynamic and oximetric changes. Because F_{NADH}/R_{365} is also independent of I_{ex}, fluctuations in effective excitation intensity caused by UV source instability or tissue movements do not affect the determination of relative NADH concentration changes.

EXPERIMENTAL

Tissue phantom

To verify the insensitivity of the F_{NADH}/R_{365} ratio to total sample absorbance (hemodynamic changes), experiments were carried out with tissue phantoms consisting of mixtures of hemoglobin in Intralipid. To determine phantom compositions with optical properties in the range of those of freshly excised rat heart, absorption and back-scattering properties of the phantoms were varied. The optical properties in the UV spectral region were determined by means of a double-integrating sphere system (Table 1).

A good correlation was found between μ_a and the hemoglobin concentration in the tissue phantoms (Table 1). μ_a did not depend on sample thickness (results not shown). The fact that a UV multiline (331, 351, 364 nm) was used may explain why μ_s' did not exactly multiply with doubling Intralipid concentration, and why μ_s' was found to decrease slightly (6 ± 3%) with increasing sample thickness (300–400 μm).

The μ_a of 100 μM hemoglobin in Intralipid (3% or 6%) corresponds to the μ_a of rat heart slabs. Heart tissue is more forward scattering than Intralipid suspensions ($\mu_s' = 1.6$ mm^{-1} versus $\mu_s' > 6$ mm^{-1}). For our purposes, however, differences in μ_s' are not important as long as criterion 1b (see above) is fulfilled (for heart tissue: $d/\partial \geq 10.4$).

Fig. 2 *A* demonstrates the linearity between NADH concentration and F_{NADH}/R_{365} ratio over the physiological NADH concentration range in tissue phantoms composed of Intralipid 3% and 50 μM hemoglobin. The positive intercept of the fluorescence axis is caused by Intralipid, which

TABLE 1 Absorption coefficient μ_a and reduced scattering coefficient $\mu_s' = \mu_s(1 - g)$ in the UV spectral region (331, 351, 364 nm) determined with a double-integrating sphere system for an intervening sample of thickness t (see Materials and Methods)

Preparation	t (μm)	Hemoglobin (μM)	μ_a (mm^{-1})	$(1 - g)\,\mu_s$ (mm^{-1})
Heart (n = 9)	427 ± 45	—	2.3 ± 0.5	1.6 ± 0.2
Blood hematocrit 2.5%*				
HbO_2#	500	—	2.1 ± 0.1	0.27 ± 0.01
Hb§	500	—	3.2 ± 0.1	0.18 ± 0.01
Blood hematocrit 5.4%*				
HbO_2#	500	—	4.6 ± 0.01	0.31 ± 0.08
Hb§	500	—	6.4 ± 0.1	0.26 ± 0.01
Intralipid 3%	400	50	1.10 ± 0.01	6.93 ± 0.08
		100	2.23 ± 0.02	6.86 ± 0.04
		200	4.49 ± 0.06	6.82 ± 0.07
Intralipid 6%	400	50	1.15 ± 0.02	12.77 ± 0.12
		100	2.23 ± 0.03	12.59 ± 0.12
		200	4.54 ± 0.03	12.21 ± 0.01

*Rat blood was diluted in Tyrode solution supplemented with 1% BSA.
#HbO_2, oxygenated blood, equilibrated with 95% O_2/5% CO_2.
§Hb, deoxygenated blood, equilibrated with 95% N_2/5% CO_2.

also fluoresces around 470 nm upon excitation with UV light.

F_{NADH}/R_{365} as a function of total sample absorbance is shown in Fig. 2 *B*. As expected from Eqs. 3 and 4, stability of the F_{NADH}/R_{365} ratio improves with increasing sample absorbance. Only for tissue phantoms containing less than 65 μM hemoglobin, with absorption coefficients significantly smaller than the μ_a of virtually bloodless rat heart, does the F_{NADH}/R_{365} ratio deviate more than 5% from the stable value reached at higher values of μ_a. Similar results were obtained with phantoms containing Intralipid 6% and with whole blood instead of purified hemoglobin.

Rat heart

The validity of the F_{NADH}/R_{365} ratio, as a suitable measure for semiquantitative fluorimetry, was tested for isolated rat heart preparations that were subjected to hemodynamic and oximetric challenges. An example of NADH fluorescence and UV reflectance images of a *blood*-perfused rat heart obtained with the biprism configuration is shown in Fig. 3.

To illustrate the potential of NADH fluorimetry and the importance of imaging, an example is given in which a rat heart showing a heterogeneous fluorescence pattern was subjected to hemodynamic and oximetric challenges. Such heterogeneity in NADH fluorescence intensity was occasionaly observed in *blood*-perfused rat hearts, which otherwise appeared normal. Fig. 4 shows the NADH fluorescence image of such a heart. In these particular heart preparations local differences in cellular energy metabolism had resulted in highly fluorescent and weakly fluorescent tissue areas. Whereas NADH fluorescence intensities of weakly fluorescent, normoxic, tissue areas did reflect changes in perfusion pO_2, NADH fluorescence intensities of highly fluorescent tissue areas did not change when the O_2 supply was interrupted (see below).

FIGURE 3 An example of UV reflectance (*left*) and NADH fluorescence (*right*) images of *blood*-perfused rat heart obtained with the biprism configuration.

FIGURE 4 NADH fluorescence image of a *blood*-perfused rat heart with a heterogeneous fluorescence pattern recorded with the videofluorimeter described by Coremans et al. (1993) and Ince et al. (1993).

Using the biprism configuration of Fig. 1, changes in NADH fluorescence and UV reflectance intensities of a highly fluorescent and a weakly fluorescent normoxic tissue area have been measured in response to hemodynamic and oximetric challenges according to protocol II (see Materials and Methods and Fig. 5).

When oxygenated *blood* is replaced by an oxygenated Tyrode solution, a marked and reproducible increase in both fluorescence and UV reflectance intensity is observed due to decreased absorption of fluorescence excitation and emission light by blood pigments—a hemodynamic effect *in extremis*. Comparison of the kinetics of the UV reflectance change in weakly fluorescent tissue (Fig. 5 *D*) with those in relatively highly fluorescent tissue (Fig. 5 *E*) does not reveal any differences, indicating that the two tissue areas were equally well perfused. During the Tyrode flushes the F_{NADH}/R_{365} ratio of highly fluorescent tissue remained constant (Fig. 5 *E*). In normoxic tissue the F_{NADH}/R_{365} ratio remained unchanged during the first 15 s of the Tyrode flush. In this time interval most erythrocytes are washed out of the microcirculation. Hereafter, apparently some metabolic change occurred, because the F_{NADH}/R_{365} ratio dropped slightly; NADH fluorescence intensity declined, whereas diffuse UV reflectance intensity remained virtually constant (Fig. 5 *D*). In any case, it is clear that the F_{NADH}/

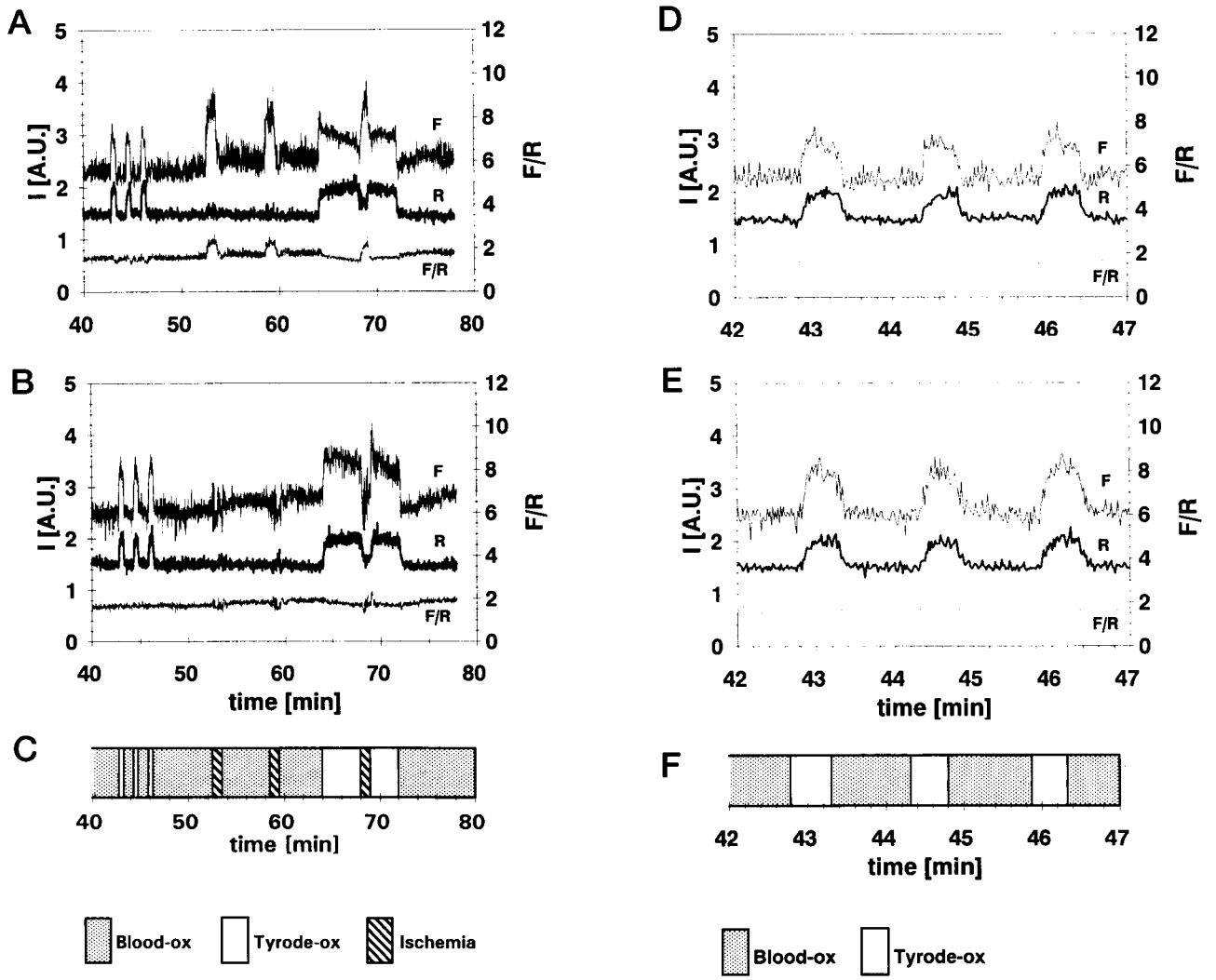

FIGURE 5 Effect of hemodynamic and/or oximetric changes on F_{NADH} (*top trace*), R_{365} (*middle trace*), and F_{NADH}/R_{365} (*bottom trace*) intensities of a weakly fluorescent, normoxic, tissue area (*A*, *D*) and a highly fluorescent, relatively hypoxic, tissue area (*B*, *E*) of a *blood*-perfused rat heart showing a heterogeneous NADH fluorescence image. Substitution of oxygenated Tyrode for *blood* and interruption of coronary perfusion were performed according to protocol II (see Materials and Methods). (*A*, *B*) Full trace; (*D*, *E*) details of Tyrode flushes; (*C*, *F*) schematic representation of relevant parts of protocol II. A.U., Arbitrary units.

R_{365} ratio provides adequate compensation for hemodynamic changes.

After the Tyrode flushes, *blood* perfusion of the heart was repeatedly interrupted, inducing both hemodynamic and oximetric changes. In weakly fluorescent normoxic tissue, interruption of the *blood* supply resulted in NADH accumulation as a consequence of insufficient O_2 supply to the mitochondria (Fig. 5 *A*). Surface NADH fluorescence intensities of the highly fluorescent tissue area did not vary with changes in the perfusion pO_2, induced by occlusion of the coronary perfusion (Fig. 5 *B*). The absence of significant changes in the UV reflectance intensity, in both normoxic and highly fluorescent tissue areas, indicates that oximetric and hemodynamic effects cancelled out at the excitation wavelength.

After the Tyrode flushes and occlusion of the coronary perfusion, the *blood* perfusion was replaced by perfusion with oxygenated Tyrode for a longer time interval. As expected, the switch to Tyrode evoked an change in fluorescence and reflectance intensities identical to that of the earlier flushes. For the highly fluorescent tissue area, occlusion of the salt perfusion resulted in a decrease in both NADH fluorescence and UV reflectance intensities, which is mainly caused by shrinkage of the heart. Despite the marked changes in fluorescence and UV reflectance during the protocol, the F_{NADH}/R_{365} ratio of this highly fluorescent tissue area remained practically constant during all interventions (Fig. 5 *B*). In normoxic tissue, cessation of the oxygenated Tyrode supply resulted in a distinct increase in NADH fluorescence intensity and a concomitant decrease in UV reflectance intensity. During the anoxic periods, caused by interruption of either *blood* or Tyrode perfusion, the F_{NADH}/R_{365} ratio appeared to stabilize at the same value (Fig. 5 *A*).

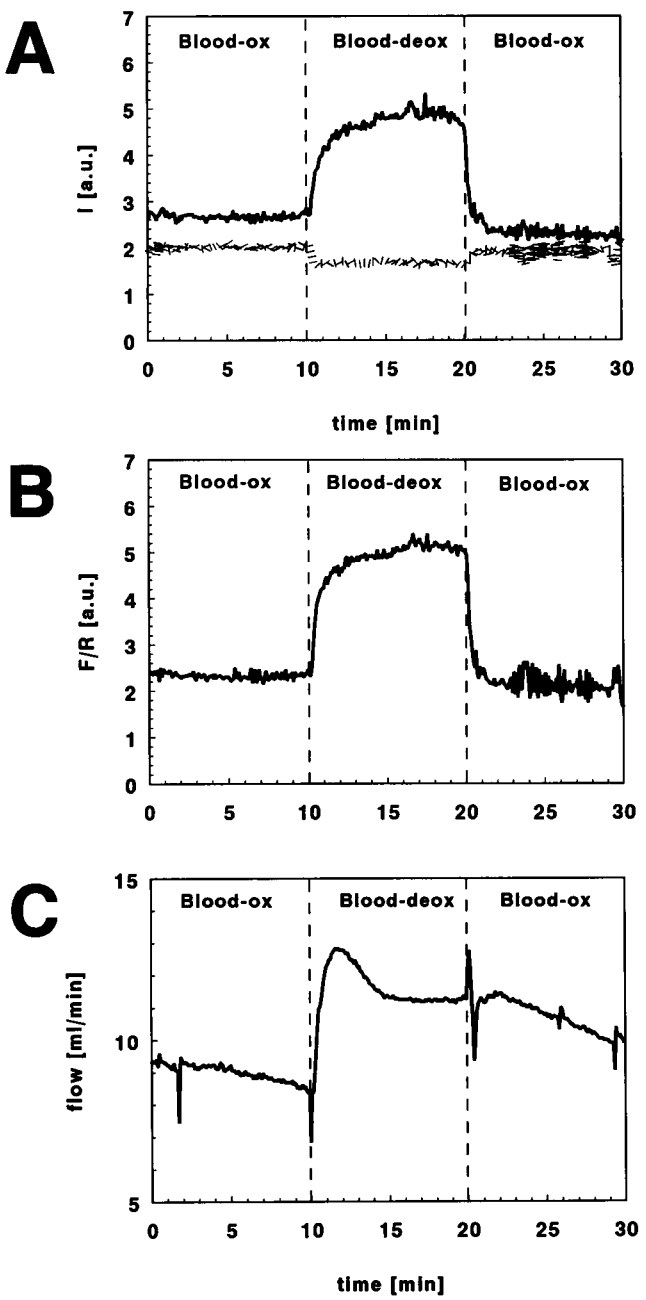

FIGURE 6 Effect of hemodynamic and oximetric changes on (*A*) F_{NADH} (*top trace*), R_{365} (*bottom trace*), and (*B*) F_{NADH}/R_{365} intensities of isolated rat heart, when compensatory vasodilation is induced by perfusion with deoxygenated *blood* according to protocol III (see Materials and Methods). (*C*) Corresponding coronary flow. A.U., Arbitrary units.

This example clearly shows that the F_{NADH}/R_{365} ratio can be used to discriminate between tissue areas with different oxidative metabolism, in spite of disturbing hemodynamic and oximetric effects. Changes in measured F_{NADH} due to effects other than changes in NADH concentration are adequately compensated for by changes in R_{365}.

When oxygenated *blood* is replaced with deoxygenated *blood*, a combination of hemodynamic and oximetric effects is induced (Fig. 6). To estimate the relative effects of compensatory vasodilation and *blood* oxygenation changes on NADH fluorescence and UV reflectance intensities of isolated rat heart, protocol III was performed. During perfusion with deoxygenated *blood*, accumulation of reducing equivalents at the high-energy side of the respiratory chain is reflected by an increase in NADH fluorescence intensity (Fig. 6 *A*). Because of compensatory vasodilation, the flow in the coronary circulation increased by 53% (Fig. 6 *C*). The absorption coefficient of deoxygenated hemoglobin (and myoglobin) at the excitation wavelength exceeds that of oxygenated hemoglobin (and myoglobin). In this case, both hemodynamic and oximetric changes contributed to increased absorption of excitation light, causing a drop in UV reflectance intensity of approximately 18% ($\Delta R_{365} = -17.8 \pm 2.1\%$, $n = 5$) (Fig. 6 *A*).

Comparison of the kinetics of UV reflectance intensity and coronary flow changes revealed that the oximetric effect on the UV reflectance change largely exceeded the hemodynamic effect. Upon substitution of deoxygenated *blood* for oxygenated *blood*, UV reflectance intensity dropped immediately to a new baseline, whereas the coronary flow increase was relatively slow. Conversely, immediate recovery of the reflectance intensity was observed upon reoxygenation, in spite of sustained increased coronary flow.

Fig. 7 compares the NADH fluorescence and reflectance changes of rat heart accompanying hypoxic hypoxia of two extremes: in vivo for hematocrit 40.8% (protocol IV) and in

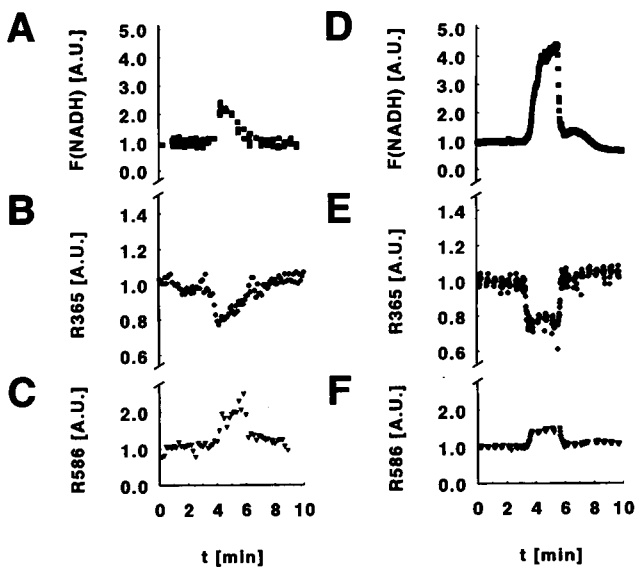

FIGURE 7 Effect of hypoxic hypoxia on F_{NADH} (■), R_{365} (●), and R_{586} (▼) intensities of (*A–C*) rat heart in vivo (hematocrit 40.8%), where O_2 in the respiratory mixture is replaced by N_2 according to protocol IV (see Materials and Methods), and (*D–F*) Tyrode-perfused isolated rat heart, where oxygenated Tyrode is replaced by deoxygenated Tyrode according to protocol I (see Materials and Methods). The NADH fluorescence and reflectance traces are aligned such that the start of each metabolic challenge corresponds to $t = 3$ min on the time axis. A.U., Arbitrary units.

vitro for Tyrode-perfused isolated heart (protocol I). The screening effect of the blood pigments on the relative fluorescence change in vivo is evident (Fig. 7, *A* and *B*). Although the kinetics differed, the UV reflectance change in blood-perfused heart (−18%, Fig. 6 *A*; −19%, Fig. 7 *B*) was comparable to the UV reflectance reduction of 23% (Fig. 7 *E*) induced by substitution of deoxygenated Tyrode for oxygenated Tyrode. Because the UV reflectance signal of cardiac tissue is largely determined by myoglobin, and hemoglobin and myoglobin have similar spectroscopic properties in the UV region, the presence of erythrocytes in the microcirculation has little effect on the relative UV reflectance change during hypoxia.

In Tyrode-perfused heart, diffuse reflectance measurements carried out at 586 nm (isosbestic wavelength hemoglobin) showed increased reflection during hypoxic hypoxia, which is most likely due to an oximetric effect of heart tissue (Fig. 7 *F*). Even in vivo, hypoxic hypoxia is accompanied by increased 586-nm reflectance, despite a possible microcirculatory blood volume increase (Fig. 7 *C*).

DISCUSSION

In the literature, selection criteria for the most accurate reflectance wavelength to compensate for hemodynamic and oximetric effects on the NADH fluorescence signal have been discussed at length. Nevertheless, discrepancies in results and interpretation remain. This is mainly because methods designed for a specific tissue type, focusing on compensation of either hemodynamic (Dóra et al., 1984; Harbig et al., 1976; Ji et al., 1977; Jöbsis et al., 1971; Mayevsky and Chance, 1974, 1982; Mayevsky et al., 1987) or oximetric (Ji et al., 1979; Kobayashi et al., 1971) effects, have been applied to experimental systems with properties different from those for which they were developed. In choosing 586 nm as the most suitable reflectance wavelength (isosbestic point of hemoglobin), Renault neglected the oximetric effect of heart tissue, arguing that the spectroscopic properties of hemoglobin and myoglobin are indistinguishable with the optical filters used in the laser fluorimeter (Renault et al., 1984). We did observe, however, a significant contribution of an oximetric effect to the 586-nm reflectance measurement (Fig. 7 *C*). Although the absorption spectra of the oxygenated and deoxygenated derivatives of hemoglobin and myoglobin have similar lineshapes, the spectra differ significantly in the position of absorption bands and isosbestic points (Antonini and Brunori, 1971). A wavelength of 586 nm is approximately halfway between the maximum absorption difference of the oxygenated and deoxygenated forms of myoglobin (581/582 nm) and its isosbestic point (592 nm). Because of the steepness of the (MbO_2-Mb) difference spectrum in this spectral region, small changes in monitoring wavelength result in large changes in the absorption difference. Moreover, the maximum absorption difference and the isosbestic point in the absorption difference spectrum of aerobic minus anaerobic suspensions of cardiac myocytes coincide with the spectral features of myoglobin (Wittenberg and Wittenberg, 1985). Therefore, the observed increase in reflectance of heart tissue at 586 nm caused by hypoxic hypoxia is most likely due to deoxygenation of myoglobin. Compensation of the blue fluorescence with red reflectance (720 nm: another isosbestic point hemoglobin), as proposed by Kobayashi et al. (1971), introduces another source of error by probing different tissue volumes due to the wavelength dependence of light propagation in tissue. Moreover, in blood-perfused organs, where metabolic changes can be accompanied by appreciable changes in blood volume, the existence of suitable (stable) isosbestic wavelengths is unlikely. Therefore, compensation methods that rely on the existence of isosbestic wavelengths, whether in reflectance spectroscopy or in isosbestic fluorimetry, are error prone.

Use of 365-nm diffuse reflectance as the reference signal has been subject to discussion because of the fact that at this wavelength the absorption characteristics of pigments in blood and tissue depend on the metabolic state (Antonini and Brunori, 1971). However, it is irrelevant which effects underly a change in tissue absorbance of UV excitation light, as long as its effect on NADH fluorescence intensity is amply compensated for.

The results presented in this paper show that the NADH fluorescence/UV reflectance ratio provides a good measure for (semi-)quantitative analysis of tissue NADH concentration, unaffected by oximetric or hemodynamic effects. In heart tissue, the conditions that have to be fulfilled for validity of the theoretical approach of the F_{NADH}/R_{365} ratio are easily satisfied. Because of the strong absorption of blood and tissue in the near-UV region, the optical penetration depth for diffuse 365-nm light is only a few hundred microns ($\delta \approx 200$ μm) (Chance et al., 1965; Ji et al., 1977), and all excitation light is absorbed or scattered in superficial tissue layers of the myocardial wall ($d \approx 2$ mm (Kanaide et al., 1982)). Because NADH fluorescence has a large Stokes shift (Lakowicz, 1983), NADH self-absorption within the sample can be ignored. Incorporation of the unknown scattering term S, the fluorescence quantum yield ϕ, and instrument characteristic G in constant C of Eq. 5 makes the F_{NADH}/R_{365} ratio a (semi-)quantitative measure for NADH fluorimetry. This is shown for tissue phantoms in Fig. 2, where a linear relationship between NADH concentration and the F_{NADH}/R_{365} ratio was found over the complete physiological NADH concentration range from 20–25 μM during normoxia to 300–450 μM during anoxia (Bessho et al., 1989; Chance et al., 1965; Katz et al., 1987).

Subtraction of the UV reflectance signal from the fluorescence signal ($F_{NADH} - k \cdot R_{365}$) has frequently been used to correct measured NADH fluorescence intensities of the cerebral cortex (Dóra et al., 1984; Harbig et al., 1976; Ji et al., 1977, 1979; Jöbsis et al., 1971; Kovach et al., 1977; Mayevsky and Chance, 1974, 1982; Mayevsky et al., 1987), but application to in vivo heart models has also been reported (Osbakken, 1994). For compensation of hemodynamic effects on NADH fluorescence intensities, this

($F_{NADH} - k \cdot R_{365}$) correction was found to be suitable for most brain preparations (Harbig et al., 1976; Jöbsis et al., 1971; Mayevsky and Chance, 1982). However, this method provides inadequate correction for oximetric effects in cerebrocortical fluorimetry (Kovach et al., 1977). Although Kramer and Pearlstein (1979) argued that algebraic subtraction of the reflectance from the NADH fluorescence is inappropriate and a ratio technique should be used instead, studies based on fluctuations in the intensity of UV reflectance of a small tissue area yielded inconsistent results. Sometimes an increase in UV reflectance intensity was observed during hypoxia of brain cortex (Ji et al., 1979), whereas in similar experimental protocols the UV reflectance decreased (Dóra et al., 1984; Harbig et al., 1976; Ji et al., 1977; Mayevsky and Chance, 1982). The issue is obscured by the fact that these investigators have all used microscopic and fiber optic techniques that suffer from an unpredictable contribution of specular reflection and cannot discriminate between spatial heterogeneity and temporal changes. Although the intensity of specularly reflected light is sensitive to tissue movement, it is not suitable to compensate movement artefacts in NADH fluorimetry. This is due to the fact that specularly reflected light is reflected directly at the air-tissue interface, whereas fluorescent light is only emitted after absorption- and scattering-induced radiation transfer phenomena (Brandes et al., 1992). Because specularly reflected light does not relate to hemodynamic and/or oximetric changes, contamination of diffuse reflectance measurements with specular reflection should be avoided. In our optical configuration the problem of specular reflection is avoided by using two crossed polarizers. The small (10°) angle between excitation and detection beams (Fig. 1) ascertains that total transmission of polarized excitation light by the analyzer is constant over the filter surface and never exceeds 0.005%. Application of "the polarization principle" to obtain a true diffuse reflectance measurement has been recognized before (Brandes et al., 1992), but has not been put into practice.

Because NADH fluorescence and UV reflectance images are measured simultaneously and image-processing software allows identification and analysis of identical tissue areas in the fluorescence and reflectance image, the F_{NADH}/R_{365} ratio is disturbed neither by motion nor by possible spatial heterogeneity of the heart surface (Ashruf et al., 1995; Barlow and Chance, 1976; Ince et al., 1993; Steenbergen et al., 1977; Williamson et al., 1982). Moreover, with a CCD imaging system, NADH fluorimetry is truly noninvasive, because no direct contact between instrumentation and tissue is needed. Another important advantage of the F_{NADH}/R_{365} ratio over other compensation methods is that the F_{NADH}/R_{365} ratio does not depend on instrument settings and does not require internal calibration. Furthermore, the uranyl calibration glass, which served to enable correction of images for fluctuations in the intensity of the light source in the experimental set-up used for Fig. 4, is no longer necessary when the F_{NADH}/R_{365} ratio technique is used.

In accordance with the tissue phantom data (Fig. 2), the F_{NADH}/R_{365} ratio in a metabolically stable heart is independent of the erythrocyte concentration in the perfusate (Fig. 5). The hemodynamic effect induced by autoregulation is more difficult to control. Compensatory vasodilation is accompanied by pronounced coronary flow increase. The available literature, however, offers little information as to how this flow control is linked to microcirculatory blood volume (Ploeg, 1994). It is therefore unclear to what extent heart surface fluorescence measurements are affected by absorbance changes due to changes in microcirculatory blood volume. Nevertheless, it is clear that such an effect is small compared to the oximetric effect of hemoglobin (Fig. 6).

The decrease in the F_{NADH}/R_{365} ratio that was observed when the perfusate of the isolated heart preparation was switched from oxygenated *blood* to oxygenated Tyrode is probably related to a metabolic and vascular response (Fig. 5). Although the O_2-carrying capacity of an oxygenated erythrocyte suspension exceeds that of oxygenated Tyrode solution, myocardial perfusion with oxygenated Tyrode apparently increases sufficiently in this non-working heart preparation to compensate for the decrease in arterial oxygen content (Buckberg and Brazier, 1975; Olders et al., 1990; Priebe, 1981; Race et al., 1967).

In *blood*-perfused heart the absence of significant changes in the UV reflectance intensity during ischemia (Fig. 5, *A* and *B*) implies that the 365-nm reflectance change associated with a possible decrease in microcirculatory *blood* volume and with oximetric effects of *blood* and tissue (deoxygenation of hemoglobin, myoglobin, reduction cytochromes) cancels out. Because the muscle tone of the myocardium increases with increasing viscosity of the perfusate, ischemia-induced tissue shrinkage is more pronounced during interruption of Tyrode perfusion. As could be expected, compression of tissue that is unresponsive to changes in O_2 supply decreases both NADH fluorescence and UV reflectance intensities (Fig. 5 *B*). Significant qualitative variations in UV reflectance changes during ischemia that have been reported in the literature can probably be attributed to contributions of specular reflection (Dóra et al., 1984; Ji et al., 1977, 1979; Mayevsky and Chance, 1982; Mills et al., 1977).

In summary, the F_{NADH}/R_{365} ratio provides a suitable measure for (semi-)quantitative NADH fluorimetry under the following conditions:

1. The penetration depth of the UV excitation light is small, so that remitted excitation light and evoked NADH fluorescence light leave the same organ face.

2. The physiological phenomena accompanying metabolic changes should not significantly alter tissue absorption of NADH fluorescence light.

The superficial nature of the fluorescence technique as dictated by condition 1 poses a disadvantage of NADH fluorimetry as monitor of the mitochondrial redox state. On the other hand, oxygenation at the tissue surface is often a good indicator of the condition of an organ. We have

illustrated the potential of NADH videofluorimetry to delineate areas with a distinct metabolic state in heart, but application of the F_{NADH}/R_{365} ratio technique to the study of oxidative metabolism is certainly not limited to the heart.

The authors thank J. F. Ashruf MD, J. P. van der Sluijs MD, A. J. Pijl MD, and M. van Aken for assistance with the blood perfusion experiments. The hospitality of Dr. G. W. Lucassen and Dr. H. J. C. M. Sterenborg from the Laser Centre (Academic Medical Centre, University of Amsterdam), where the double-integrating sphere measurements were performed with the assistance of P. L. T. M. Frederix, is gratefully acknowledged.

This study was supported in part by the Netherlands Heart Foundation (grant 90.298).

REFERENCES

Alexander, B., T. von Arnem, M. Aslam, P. S. Kohle, and I. S. Benjamin. 1984. Methods in laboratory investigation. Practical miniaturized membrane oxygenator for isolated organ perfusion. *Lab. Invest.* 50:597–603.

Antonini, E., and M. Brunori. 1971. Hemoglobin and Myoglobin in Their Reactions with Ligands. North Holland Publishing Company, Amsterdam. 14.

Ashruf, J. F., J. M. C. C. Coremans, H. A. Bruining, and C. Ince. 1995. Increase of cardiac work is associated with decrease of mitochondrial NADH. *Am. J. Physiol.* 269:H856–H862.

Austin, G., R. Jutzy, B. Chance, and C. Barlow. 1978. Noninvasive monitoring of human brain oxidative metabolism. *In* Frontiers of Biological Energetics. D. L. Dutton, J. S. Leigh, and A. Scapa, editors. Academic Press, New York. 1445–1455.

Avi-Dor, Y., J. M. Olson, M. D. Doherty, and N. O. Kaplan. 1962. Fluorescence of pyridine nucleotides in mitochondria. *J. Biol. Chem.* 237:2377–2383.

Barlow, C. H., and B. Chance. 1976. Ischemic areas in perfused rat hearts: measurement by NADH fluorescence photography. *Science.* 193: 909–910.

Bessho, M., T. Tajima, S. Hori, T. Satoh, K. Fukuda, S. Kyotani, Y. Ohnishi, and Y. Nakamura. 1989. NAD and NADH values in rapidly sampled dog heart tissues by two different extraction methods. *Anal. Biochem.* 182:304–308.

Brandes, R., V. M. Figueredo, S. A. Camacho, B. M. Massie, and M. W. Weiner. 1992. Suppression of motion artifacts in fluorescence spectroscopy of perfused hearts. *Am. J. Physiol.* 263:H972–H980.

Buckberg, G., and J. Brazier. 1975. Coronary blood flow and cardiac function during hemodilution. *Bibl. Haematol.* 41:173–189.

Chance, B., P. Cohen, F. Jöbsis, and B. Schoener. 1962. Intracellular oxidation-reduction states in vivo. The microfluorimetry of pyridine nucleotide gives a continuous measurement of the oxidation state. *Science.* 137:499–508.

Chance, B., and B. Thorell. 1959. Localization and kinetics of reduced pyridine nucleotides in living cells by microfluorometry. *J. Biol. Chem.* 234:3044–3050.

Chance, B., J. R. Williamson, D. Jamieson, and B. Schoener. 1965. Properties and kinetics of reduced pyridine nucleotide fluorescence of the isolated and in vivo rat heart. *Biochem. Z.* 341:357–377.

Coremans, J. M. C. C., C. Ince, and H. A. Bruining. 1993. NADH fluorimetry and diffuse reflectance spectroscopy on rat heart. *In* Medical Optical Tomography: Functional Imaging and Monitoring, Vol. IS 11. G. Müller, B. Chance, R. Alfano, S. Arridge, J. Beuthan, E. Gratton, M. Kaschke, B. Masters, S. Svanberg and P. van der Zee, editors. SPIE Optical Engineering Press, Washington, DC. 589–617.

Deyl, Z., R. Praus, H. Sulcová, and J. N. Goldman. 1969. Fluorescence of collagen. Properties of tyrosine residues and another fluorescent element in calf skin collagen. *FEBS Lett.* 5:187–191.

Dóra, E., L. Gyulai, and A. G. B. Kovách. 1984. Determinants of brain activation-induced cortical NAD/NADH responses in vivo. *Brain Res.* 299:61–72.

Duboc, D., G. Renault, J. Poliansky, M. Muffat-Joly, M. Toussaint, F. Guerin, J. J. Pocidalo, and M. Fardeau. 1987. NADH measured by laser fluorimetry in skeletal muscle in McArdle's disease. *N. Engl. J. Med.* 316:1664–1665.

Duboc, D., M. Toussaint, D. Donsez, S. Weber, F. Guerin, M. Degeorges, G. Renault, J. Poliansky, and J. J. Pocidalo. 1986. Detection of regional myocardial ischaemia by NADH laser fluorimetry during human left heart catheterisation. *Lancet.* 2:522.

Eisinger, J., and J. Flores. 1979. Front-face fluorometry of liquid samples. *Anal. Biochem.* 94:15–21.

Eng, J., R. M. Lynch, and R. S. Balaban. 1989. Nicotinamide adenine dinucleotide fluorescence spectroscopy and imaging of isolated cardiac myocytes. *Biophys. J.* 55:621–630.

Estabrook, R. W.. 1962. Fluorometric measurement of reduced pyridine nucleotide in cellular and subcellular particles. *Anal. Biochem.* 4:231–245.

Flock, S. T., S. L. Jacques, B. C. Wilson, W. M. Star, and M. J. C van Gemert. 1992. Optical properties of Intralipid: A phantom medium for light propagation studies. *Lasers Surg. Med.* 12:510–519.

Hamilton, R. L., M. N. Berry, M. C. Williams, and E. M. Severinghaus. 1974. A simple and inexpensive membrane "lung" for small organ perfusion. *J. Lipid Res.* 15:182–186.

Harbig, K., B. Chance, A. G. B. Kovách, and M. Reivich. 1976. In vivo measurement of pyridine nucleotide fluorescence from cat brain cortex. *J. Appl. Physiol.* 41:480–488.

Heineman, F. W., and R. S. Balaban. 1990. Effects of afterload and heart rate on NAD(P)H redox state in the isolated rabbit heart. *Am. J. Physiol.* 264:H433–H440.

Heinrich, U., J. Hoffmann, and D. W. Lübbers. 1987. Quantitative evaluation of optical reflection spectra of blood-free perfused guinea pig brain using a nonlinear multicomponent analysis. *Pflügers Arch.* 409: 152–157.

Hoffmann, J., U. Heinrich, H. R. Ahmad, and D. W. Lübbers. 1984. Analysis of tissue reflection spectra obtained from brain or heart, using the two flux theory for non-constant light scattering. *Adv. Exp. Med. Biol.* 180:555–563.

Hoffmann, J., R. Wodick, F. Hannebauer, and D. W. Lübbers. 1983. Quantitative analysis of reflection spectra of the surface of the guinea pig brain. *Adv. Exp. Med. Biol.* 169:831–839.

Ince, C., J. F. Ashruf, J. A. M. Avontuur, P. A. Wieringa, J. A. E. Spaan, and H. A. Bruining. 1993. Heterogeneity of the hypoxic state in the rat heart is determined at capillary level. *Am. J. Physiol.* 264:H294–H301.

Ince, C., and H. A. Bruining. 1991. Optical spectroscopy for the measurement of tissue hypoxia. *In* Update in Intensive Care and Emergency Medicine: Update 1991. J. L. Vincent, editor. Springer-Verlag, Berlin. 161–171.

Ince, C., J. M. C. C. Coremans, and H. A. Bruining. 1992. In vivo NADH fluorescence. *Adv. Exp. Med. Biol.* 317:277–296.

Ishimaru, A. 1978. Wave Propagation and Scattering in Random Media, Vol. 1. New York, Academic Press.

Ji, S., B. Chance, K. Nishiki, T. Smith, and T. Rich. 1979. Micro-light guides: a new method for measuring tissue fluorescence and reflectance. *Am. J. Physiol.* 236:C144–C156.

Ji, S., B. Chance, B. H. Stuart, and R. Nathan. 1977. Two dimensional analysis of the redox state of the rat cerebral cortex in vivo by NADH fluorescence photography. *Brain Res.* 119:357–373.

Jöbsis, F. F., and J. C. Duffield. 1967. Oxidative and glycolytic recovery metabolism in muscle. *J. Gen. Physiol.* 50:1009–1047.

Jöbsis, F. F., M. O'Connor, A. Vitale, and H. Vreman. 1971. Intracellular redox changes in functioning cerebral cortex. I. Metabolic effects of epileptiform activity. *J. Neurophysiol.* 34:735–749.

Kanaide, H., R. Yoshimura, N. Makino, and M. Nakamura. 1982. Regional myocardial function and metabolism during acute coronary artery occlusion. *Am. J. Physiol* 242:H980–H989.

Katz, A., A. Edlund, and K. Sahlin. 1987. NADH content and lactate production in the perfused rabbit heart. *Acta Physiol. Scand.* 130: 193–200.

Kessler, M., and K. Frank. 1992. The Erlangen micro-lightguide spectrophotometer EMPHO 1. *In* Quantitative Spectroscopy in Tissue. K. Frank

and M. Kessler, editors. pmi Verlag, Frankfurt am Main, Germany. 61–74.

Klingenberg, M., W. Slenczka, and E. Ritt. 1959. Vergleichende Biochemie der Pyridinnucleotid-Systeme in Mitochondrien verschiedener Organe. *Biochem. Z.* 332:47–66.

Kobayashi, S., K. Nishiki, K. Kaede, and E. Ogata. 1971. Optical consequences of blood substitution on tissue oxidation-reduction state fluorometry. *J. Appl. Physiol.* 31:93–96.

Koretsky, A. P., L. A. Katz, and R. S. Balaban. 1987. Determination of pyridine nucleotide fluorescence from the perfused heart using an internal standard. *Am. J. Physiol.* 253:H856–H862.

Kovach, A. G. B., E. Dóra, A. Eke, and L. Gyulai. 1977. Effects of microcirculation on microfluorometric measurements. *In* Oxygen and Physiological Function. F. F. Jöbsis, editor. Professional Information Library, Dallas. 111–132.

Kramer, R. S., and R. D. Pearlstein. 1979. Cerebral cortical microfluorimetry at isosbestic wavelengths for correction of vascular artifact. *Science.* 205:693–696.

Kubelka, P. 1948. New contributions to the optics of intensily light-scattering materials. Part I. *J. Opt. Soc. Am.* 38:448–457.

Kubelka, P. 1954. New contributions to the optics of intensily light-scattering materials. Part II. Nonhomogeneous layers. *J. Opt. Soc. Am.* 44:330–335.

Kubelka, P., and F. Munk. 1931. Ein Beitrag zur Optik der Farbanstriche. *Z. Technische Physik.* 11:76–77.

Lakowicz, J. R. 1983. Principles of Fluorescence Spectroscopy. Plenum Press, New York. 1–18.

Mayevsky, A., and B. Chance. 1974. Repetitive patterns of metabolic changes during cortical spreading depression of the awake rat. *Brain Res.* 65:529–533.

Mayevsky, A., and B. Chance. 1982. Intracellular oxidation-reduction state measured in situ by a multichannel fiber-optic surface fluorometer. *Science.* 217:537–540.

Mayevsky, A., S. Nioka, and B. Chance. 1987. Fiber optic surface fluorometry/reflectometry and ^{31}P NMR for monitoring the intracellular energy state in vivo. *Adv. Exp. Med. Biol.* 222:365–374.

Mills, S. A., F. F. Jöbsis, and A. V. Seaber. 1977. A fluorometric study of oxidative metabolism in the in vivo canine heart during acute ischemia and hypoxia. *Ann. Surg.* 186:193–200.

Nuutinen, E. M.. 1984. Subcellular origin of the surface fluorescence of reduced nicotinamide nucleotides in the isolated perfused rat heart. *Basic Res. Cardiol.* 79:49–58.

Olders, J., Z. Turek, J. Evers, L. Hoofd, B. Oeseberg, and F. Kreuzer. 1990. Comparison of Tyrode and blood perfused working isolated rat hearts. *Adv. Exp. Med. Biol.* 277:403–413.

Osbakken, M. D. 1994. I-2 Metabolic regulation of in vivo myocardial contractile function: multiparameter analysis. *Mol. Cell. Biochem.* 133/134:13–37.

Pappajohn, D. J., R. Penneys, and B. Chance. 1972. NADH spectrofluorometry of rat skin. *J. Appl. Physiol.* 33:684–687.

Pickering, J. W., S. A. Prahl, N. van Wieringen, J. F. Beek, H. J. C. M. Sterenborg, and M. J. C. Gemert. 1993. Double-integrating sphere system for measuring the optical properties of tissue. *Appl. Opt.* 32: 399–410.

Ploeg, C. P. B. van der. 1994. Intramyocardial blood volume and oxygen exchange. Thesis Technische. Universiteit Delft, The Netherlands.

Ploem, J. S. 1970. Standards for fluorescence microscopy. *In* Standardization in Immunofluorescence. E. J. Holborow editor. Blackwell, Oxford. 137–153.

Prahl, S. A., M. J. C. van Gemert, and A. J. Welch. 1993. Determining the optical properties of turbid media using the adding doubling method. *Appl. Opt.* 32:559–568.

Priebe, H. J. 1981. Hemodilution and oxygenation. *Int. Anesth. Clin.* 19:237–255.

Race, D., H. Dedichsen, and W. Schenk, Jr. 1967. Regional blood flow during dextran-induced normovolemic hemodilution in the dog. *J. Thorac. Cardiovasc. Surg.* 53:578–586.

Renault, G., D. Duboc, and M. Degeorges. 1987. In situ laser fluorimetry in cardiology. *J. App. Cardiol.* 2:91–104.

Renault, G., E. Raynal, M. Sinet, M. Muffat-Joly, J.-P. Berthier, J. Cornillault, B. Godard, and J.-J. Pocidalo. 1984. In situ double-beam NADH laser fluorimetry: a choice of a reference wavelength. *Am. J. Physiol.* 246:H491–H499.

Schomacker, K. T., J. K. Frisoli, C. C. Compton, T. J. Flotte, J. M. Richter, N. S. Nishioka, and T. F. Deutsch. 1992. Ultraviolet laser-induced fluorescence of colonic tissue: basic biology and diagnostic potential. *Lasers Surg. Med.* 12:63–78.

Scott, D. A., L. W. Grotyohann, J. Y. Cheung, and R. C. Scaduto, Jr. 1994. Ratiometric methodology for NAD(P)H measurement in the perfused rat heart using surface fluorescence. *Am. J. Physiol.* 267:H636–H644.

Staveren, H. J. van, C. J. M. Moes, S. A. Prahl, and M. J. C. van Gemert. 1991. Light scattering of Intralipid 10% in the wavelength range of 400–1100 nm. *Appl. Opt.* 30:4507–4514.

Steenbergen, C., G. de Leeuw, C. Barlow, B. Chance, and J. R. Williamson. 1977. Heterogeneity of the hypoxic state in perfused rat heart. *Circ. Res.* 41:606–615.

Svaasand, L. O., and R. Ellingsen. 1983. Optical properties of human brain. *Photochem. Photobiol.* 38:293–299.

Vern, B., W. C. Whitehouse, and W. H. Schuette. 1975. Sodium fluorescein: a new reference for NADH fluorometry. *Brain Res.* 98: 405–409.

Williamson, J. R., K. N. Davis, and G. Medina-Ramirez. 1982. Quantitative analysis of heterogeneous NADH fluorescence in perfused rat hearts during hypoxia and ischemia. *J. Mol. Cell. Cardiol.* 14(Suppl. 3):29–35.

Wittenberg, B. A., and J. B. Wittenberg. 1985. Oxygen pressure gradients in isolated cardiac myocytes. *J. Biol. Chem.* 260:6548–6554.